Deuterium Gas Charging Experiments with Pd Powders for Excess Heat Evolution
(II) Discussions on Experimental Results and Underlying Physics

A.Takahashi[1*], A. Kitamura[2], T. Nohmi[2], Y. Sasaki[2],
Y. Miyoshi[2], A. Taniike[2], R. Seto[1], and Y. Fujita[1]
[1]Technova Inc. *akito@sutv.zaq.ne.jp
[2](Division of Marine Engineering, Graduate School of Maritime Sciences, Kobe University)

Our experimental results obtained for Pd/PdO/ZrO_2 nano-composite samples under the joint research of Kobe University and Technova Inc. in the 2008 fiscal year are summarized and discussed in the view of underlying physics. Arata-Zhang's excess heat result demonstrated in May 2008 was replicated quantitatively. For Pd/PdO/ZrO_2 powders (produced by Santoku Co. , Kobe Japan), we obtained:1) D-gas charge in the 1st phase (zero pressure interval) gave 20~90 % excess heat than H-gas charge. 2) In the 2nd phase of pressure rise (finally up to 1MPa), significant excess heat (about 2 kJ/g-Pd) for D-gas charge was observed, while near zero level excess heat for H-gas charge was observed. We discuss the underlying surface and nano-particle physics in views of the enhanced surface adsorption potential by fractal sub-nano-scale trapping points on nano-Pd particle, the diffusion to inner shallower Bloch potential of regular Pd lattice, and the drastic mesoscopic and isotopic effect of surface and lattice rearrangement of nano-Pd particle by full D(H)-absorption to make deeper D(H) trapping potentials of surface adsorption (about 2eV for D) and intermediate surface state trapping.

1. Introduction

The aim, experimental apparatus, experimental procedure and observed results of deuterium (and protium) gas charging experiments with various nano-fabricated Pd powders have been written in our first paper to this JCF9 meeting[1)]. The observed results for Pd/PdO/ZrO_2 nano-composite samples (about 10 nm diameter Pd particles dispersed in about 7 micron size ZrO_2 flakes) provided us very interesting performance of deuterium (D) and protium (H) absorption and exothermic energy generation.

We discuss the results to be compared with Arata-Zhang work[2)], our results with 100nm Pd particle powders and Pd-black powders. The results by nano-Pd/ZrO_2 samples are very interesting since specific surface effects in adsorption and following absorption into inner "lattice" sites look taking place to result in anomalously large stoichiometry values (x>1) of PdDx and deep trapping potential (or released energy). Compared with the results of 100nm Pd particle-powders, 10nm Pd particles dispersed in ZrO_2 are regarded to have showed the drastic mesoscopic effects with isotopic difference. We will discuss these points in the following.

2. Trend of Heat-Power Evolution

The evolutions of heat and gas-pressure can be discussed for two different phases, the 1st phase and the second phase as we show typical data in Fig.1.

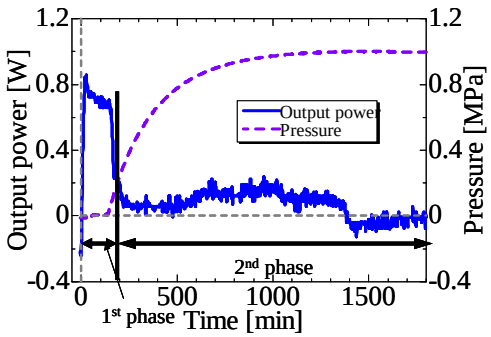

Fig.1: Typical heat (power) evolution data with Pd/ZrO$_2$ nano-composite sample with D-gas charge (D-PZ1#1 run)

The 1st phase is defined as the time-interval where reaction chamber (cell) keeps nominal "zero" gas-pressure. This means almost all D(H)-gas charged was absorbed by nano-Pd powders. Heat (power) evolution curve in the 1st phase may be regarded mostly by chemical reaction energy during D(H)-gas absorption into nano-Pd powders, in usual chemistry view. However, we may have component of "nuclear" process that we discuss later.

Trend of heat-power evolution in the second phase is very isotope dependent, as typical data is shown in Fig.2.

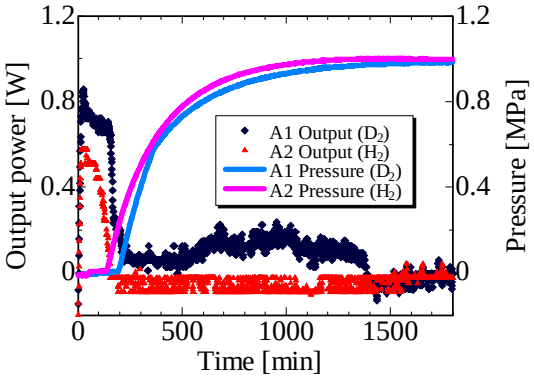

Fig.2: Typical "excess heat-power" evolution by D-charge for Pd/ZrO2 sample (D-PZ1#1run), compared with "zero" power level by H-gas charge (H-PZ2#1 run)

The H-gas charge have given "zero" power level (sometimes negative integrated values according to zero-level drift of calorimetry). Obviously, the D-gas charge to Pd/PdO/ZrO$_2$ nano-composite sample gave much more heat-power than the H-gas charge, for both phases.

3. Results and Discussions for 1st Phase Data

We summarize the integrated data of D(H)/Pd ratios, Heat per one-gram-Pd, Energy per D(H) atom absorption and gas-flow rates in **Table-1 (see end of text)**.

First we discuss the data for 100nm Pd-particle powders (D-PP and H-PP runs in Table1). Loading ratios, D(H)/Pd, are 0.43 and 0.44 respectively for deuterium (D) and protium (H) gas charging. Specific energies per absorbed D (or H) atom E_{1st} (or ΔH_s) values are 0.24eV/atom-D and 0.20eV/atom-H. When D(H) is absorbed in metal lattice, surface adsorption traps D(H) molecule (or atom) first and diffuse into inner lattice sites (O-sites of Pd, usually) gradually. Fig.3 illustrates typical form of surface trapping potential and inner periodical (Bloch) trapping potentials.

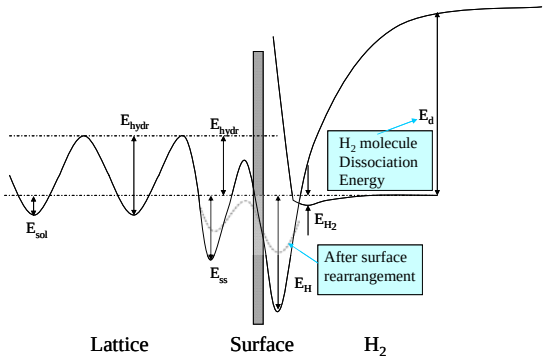

Fig.3: Image of D(H) trapping potentials at surface adsorption (depth E_H) and lattice absorption (depth E_{hydr}); trapped D(H) atom diffuses gradually into inner Bloch trapping potentials through the QM tunneling. After full loading (x=1 for PdDx), rearrangement of Pd lattice may

happen to make shallower potentials.

For known values in text book[3], E_H is about 0.5eV and E_{hydr} is 0.23eV. The difference, E_H-E_{hydr} , becomes the energy released per D(H)-atom absorption in lattice and is about 0.25eV for balk Pd lattice.

Observed E_{1st} (ΔH_s) values for 100nm Pd particle powder are near to this value of balk Pd metal. This means that 100nm Pd particle works as balk-metal for D(H) absorption.

We will see E_{1st} values for Pd-black and Pd/PdO/ZrO_2 nano-composite samples will have given much larger energies (deeper trapping potentials) to show the drastic mesoscopic effects.

Next, we look integrated data for Pd-black samples (D-PB and H-PB runs) in Table-1. E_{1st} values in averages of runs are 0.70±0.15eV/atom-D and 0.69± 0.10eV/atom-H. These values are significantly higher than the balk value about 0.25eV. For the virgin runs (#1 runs), significantly high loading as $PdD_{0.88}$ or $PdH_{0.79}$ were observed. However, for runs with used samples (#2, #3, #4 runs), loading ratios were as small as 0.23 in average. Nevertheless the specific E_{1st} values were observed as same as the virgin (#1) runs. This fact means that microscopic active adsorption sites on surface of used Pd-black are working in the same way as the virgin Pd-black sample, although effective area of active surface decreased to 1/3 or less.

We made SEM observation for Pd-black samples of "before" and "after" usage. We found the used Pd-black sample powders clumped together to be bigger sizes (about 10 times) than the virgin one and "fractal" nano-structures on surface of virgin Pd-black samples were flattened. We observed excess heat-like event in local time interval of the 1st phase data for virgin Pd-black and positive excess heat in the 2nd phase, while heat-power level dropped drastically for the used Pd-black runs (#2 run and later runs). We understand that Pd-black has good nano-structure for making anomalous "CMNS effect", but the clumping-together effect by absorbing D(H) makes the CMNS effect disable. To overcome this, we need to avoid the clumping-together effect. The clumping-together effect is not sintering, because we did not observe the clumping-together by baking Pd-black powders up to 300 deg C before #1 run.

The idea by Arata-Zhang group[2] is of dispersed Pd nano-particles (5nm diameter) in ceramics as ZrO_2 flakes to block the clumping-together effect.

Now we discuss the integrated data in the 1st phases for Pd/PdO/ZrO_2 samples (D-PZ and H-PZ runs in Table1). We observed heat-power levels were strongly dependent on the D(H) gas-flow rate. The larger gas-flow rate has trend to give larger excess heat level in the 1st phase, but the 1st phase ends earlier than the case of smaller flow rate. This is understood as the faster gas-flow meets faster saturation of D(H) absorption in powders. Therefore, to compare specific values of E_{1st} (released energy per D(H)-atom), D(H)/Pd (loading ratio) and heat (in kJ) per g-Pd is more appropriate to see the underlying physics.

Our first surprise is that all measured loading ratios, D(H)/Pd values for the 1st phases are greater than 1.0, namely overloading (x=1.1 in average for PdD(H)x stoichiometry) in usual sense, even though the background gas pressure were nearly zero (near vacuum). This must be said as the drastic mesoscopic effect of D(H) absorption by the Pd nano-coposite samples. For the known balk Pd-metal, D(H) atoms are trapped in Bloch potentials (see Fig.3) at O-sites for x<1.0. The observed anomalous data of x>1.0 should show that the additional trappings at T-sites happened

by the mesoscopic effect (about 5000 Pd atoms existing in a 5nm diameter particle).

The data for specific released energy E_{1st} values are also anomalously large and isotope (D or H)-dependent. These are 2.2-2.5eV/atom-D and 1.3-2.1eV/atom-H. Deuterium gives larger E_{1st} values. These released energy values are 5-10 times of the conventional value 0.25eV for balk Pd metal. These values are however dependent on gas-flow rate, and we need further investigation so far. As PZ samples gave drastic mesoscopic effects, compared to the 100nm Pd powder we need further study by changing nano-Pd particle size.

We take the ratios of [heat/D]/[heat/H] in 1st phases. We obtain the ratios as 1.94 to 1.3 for the first and second PZ runs. The data we deduced from Arata-Zhang's 1st phase is about 1.3. We can say our data for the first phase replicated quantitatively the Arata-Zhang result, although Arata-Zhang used 5nm diameter Pd nano-particles dispersed in ZrO_2 flakes and ours was 10nm.

4. Excess Heat for the Second Phase

As summarized in Table-1, we observed positive excess heat in the 2nd phase of D-PZ series runs for virgin (#1 run) samples (we tried three pairs of samples for simultaneous runs with D-gas by A1 (A2 for D-PZ5) and H-gas by A2 (A1 for H-PZ6) cells). For the D-PZ5 run, D-gas cylinder dried out in the 2nd phase and gas-pressure decreased (we had leakage), so that excess heat phenomenon was not observed. For earlier two PZ runs, we observed clear excess heat, only for D-gas charging, 2.27 and 2.07kJ/g-Pd in the time interval of 1600 minutes.

Arata-Zhang gave 29.2kJ with 24.4g Pd/ZrO2 sample. Assuming their sample contained 7.7g net Pd weight, we get 2.8kJ/g-Pd for 3000minutes time interval with higher D-gas pressure (10MPa maximum), after correcting specific H-absorption energy E_{1st} value (about 1eV/atom-H as we observed). We can say that our results of 2nd phase heat was comparable (or more) to Arata-Zhang's data for about two times longer time interval with higher gas-pressure.

In Fig.4, we show the rather steady excess heat evolution for used Pd/PdO/ZrO_2 samples (D-PZ3#2 and H-PZ4#2 runs).

We obtained total excess heat of 3.3 kJ/g-Pd for 9000 minutes of D-gas charging and later evacuation.

Before the end of run, we observed significant excess heat evolution after the evacuation of A1 (D-gas) cell. The expanded data is shown in Fig.5.

We speculate, the so called "heat after death event" was observed in the gas-loading experiment, also. The Santoku Pd/PdO/ZrO_2 samples retained 100 times D-atoms after the evacuation, compared to that of Pd-black, as the degassing data after evacuation and baking clearly show very interesting performance of Santoku-sample (See Fig.6).

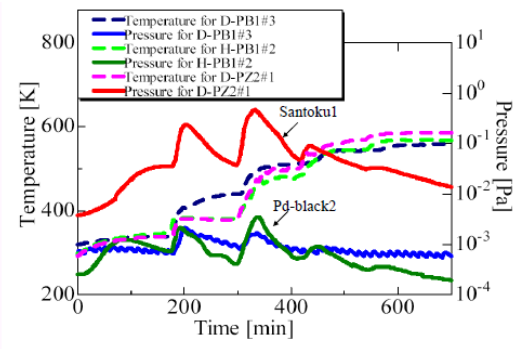

Fig.6: De-gassing data for Santoku-sample compared with that for Pd-black; Santoku-sample retains 100 times D(H)-atoms by its very deep trapping potentials of the mesoscopic effect of dispersed Pd-nano particles

The heat after death event may take place by trapped deuteron cluster (namely TSC-formation by Takahashi model[4]) at very deep (maybe about 2eV for D absorbed PZ-sample) surface adsorption potentials, where deuterons from inner Bloch trapping potentials diffuse gradually to surface trapping points to form transient 4D/TSC cluster and makes $4D \rightarrow {}^4He + {}^4He + 47.6MeV$ reactions[4] as green nuclear energy source.

Lastly, we discuss about possible chemical energy release by oxidation of charged D(H)-gas, as samples contained PdO and ZrO_2 components. Already Fig.6 shows clearly D(H)-gas was mostly absorbed by Pd in PZ samples, since Pd-black gave same pattern of degassing.

It is difficult to assume large contribution of ZrO_2 to these quantities. We have to consider reduction of PdO_x followed by production of xD_2O (xH_2O) and PdD_y (PdH_y). The reaction energies Q_D and Q_H are evaluated to be $(162.6 \times x + 70.0 \times y)$ kJ and $(156.6 \times x + 58.0 \times y)$ kJ, respectively. For assumed values of $x = 1 \sim 0$ and $y = 0 \sim 1$, Q_D and Q_H are 0.84 ~ 0.73 eV/D and 0.81 ~ 0.60eV/H, respectively. These are too small to account for both the observed E_{1st} energies and the isotope effects.

There might be an yet-unknown atomic/electronic process governing the phenomenon in the present mesoscopic system, or the concept of “atom clusters” might apply. However, it seems rather difficult to assume that such a large isotope effect is only in the electronic process of adsorption and/or hydride formation. Some nuclear process as suggested by the 4D/TSC model could be a candidate for the process responsible for the phenomenon.

5. **Concluding Remarks**

Arata-Zhang’s Excess Heat Result was replicated quantitatively by our more precise heat and loading ratio measurements.

For $Pd/PdO/ZrO_2$ powders (Santoku-samples):

1) The D-gas charge in the 1st phase (zero pressure) gave 20-90% excess heat than the H-gas charge.

2) In the 2nd phase, significant excess heat (about 2 kJ/g-Pd) for the D-gas charge, while zero level for the H-gas charge, was observed.

No increase of neutron counts was seen, neither increase of gamma-rays over natural backgrounds.

D(H)/Pd ratios in the end of 1st phase was x>1.0, namely over-loading (x=1.1 in average). Flow rate dependence of x-values should be investigated further.

Further experiments changing conditions will be fruitful for developing clean energy devices.

Nano-Pd dispersed sample (Santoku, Pd/ZrO_2) retained 100 times more D(H) atoms after evacuation, than the Pd-black case. Mesoscopic effect by Pd-nano-particle, namely surface and lattice rearrangement probably makes deep D(H) trapping potentials (1.0-2.5eV). We need study for D(H)-gas flow-rate dependence. Stable excess heat production is expected for #2 and later runs. We need further study for this. Detection of nuclear products by the B-system (we plan) is expected.

Replication by other groups is important to confirm our results.

References:

1) Y. Sasaki, A. Kitamura, T. Nohmi, Y. Miyoshi, A. Taniike, A. Takahashi, R. Seto, and Y. Fujita; Deuterium Gas Charging Experiments with Pd Powders for Excess Heat Evolution, (I) Results of absorption experiments using Pd powders, (this meeting)

2) Y. Arata and Y. Zhang: The special report on research project for creation of new energy, J. High Temperature Society, No. 1. 2008.

3) Y. Fukai, K. Tanaka, Y. Uchida: Hydrogen and Metal (in Japanese), Uchida-Roukakuho Pub., Tokyo, ISBN=4-7536-5608-X (2002)

4) A. Takahashi: Cold Fusion 2008- Mechanism of Condensed Cluster Fusion (in Japanese), Kogakusha, ISBN=978-4-7775-1361-1 (2008)

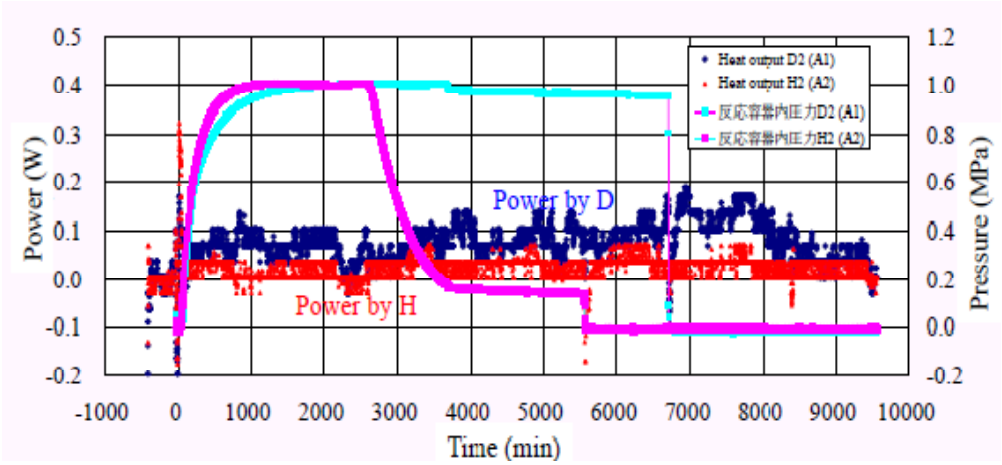

Fig.4: Long lasted excess heat evolution for used Pd/PdO/ZrO_2 sample

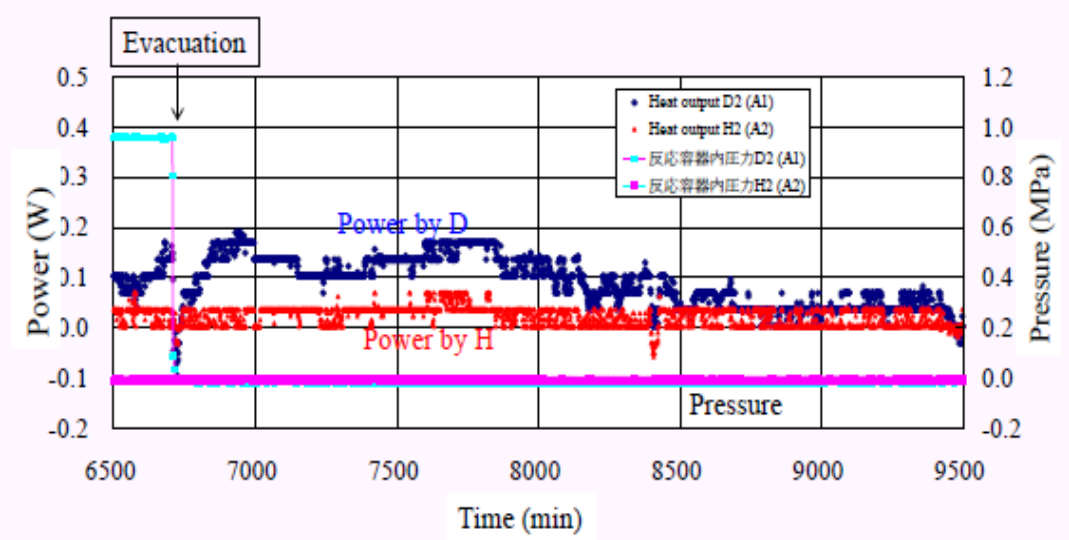

Fig.5: "Heat after death" event we observed after the evacuation of A1 (D-gas) cell for D-PZ2#2 run

Table1: Summary of Integrated Data for phase-1 and phase-2, comparing 100nm Pd powder, Pd-black and Pd/Zr nano-composite samples.

Run #	weight of Pd [g]	Flow rate [sccm]	Output energy [kJ]		Specific output energy [kJ/g]		D/Pd or H/Pd (1st ph.)	E1st [eV/D(H)]
			1st phase	2nd phase	1st phase	2nd phase		
D-PP1#1	5.0	2.7	0.5±0.4	2.5±4.1	0.10±0.07	0.52±0.83	0.43	0.26±0.14
D-PP1#2	5.0	3.8	0.5±0.2	4.0±4.4	0.10±0.05	0.79±0.88	0.44	0.25±0.09
H-PP2#1	5.0	5.4	0.4±0.2	2.6±3.9	0.08±0.03	0.53±0.80	0.44	0.20±0.07
D-PB1#1	3.2	3.6	1.7±0.3	8.3±4.5	0.54±0.10	2.60±1.40	0.88	0.67±0.12
H-PB2#1	3.6	4.2	1.6±0.3	**(-2.2±4.6)**	0.45±0.08	**(-0.62±1.30)**	0.79	0.62±0.11
D-PB3#1	20.0	2.9	9.3±1.1	1.1±0.5	0.47±0.06	0.06±0.02	0.79	0.65±0.08
D-PB3#2	20.0	0.9	3.3±0.5	3.4±2.6	0.17±0.03	0.17±0.13	0.23	0.79±0.05
H-PB3#3	20.0	2.1	3.2±0.2	14±4.6	0.16±0.01	0.68±0.24	0.24	0.74±0.05
D-PZ1#1	3.0	1.8	7.0±0.2	6.8±1.3	2.33±0.05	2.27±0.43	1.08	2.4±0.05
H-PZ2#1	3.0	2.3	3.6±0.1	**(-5.1±1.4)**	1.20±0.02	**(-1.70±0.47)**	1.00	1.3±0.02
D-PZ3#1	3.0	1.9	6.4±0.2	6.2±1.4	2.13±0.05	2.07±0.47	1.08	2.2±0.05
H-PZ4#1	3.0	3.6	4.8±0.1	1.9±1.4	1.60±0.02	0.63±0.47	0.86	2.1±0.03
D-PZ5#1	3.0	2.0	7.1±0.2	1.3±1.4	2.38±0.03	0.42±0.45	1.04	2.5±0.03
H-PZ6#1	3.0	5.9	7.1±0.1	**(-0.2±1.4)**	2.36±0.02	**(-0.08±0.48)**	1.34	1.9±0.02
Average for PZ		**(D)**	6.9±0.4	4.8±3.0	2.3±0.1	1.6±1.0	1.1±0.0	2.4±0.2
		(H)	5.2±1.8	**(-1.1±3.6)**	1.7±0.6	**(-0.4±1.2)**	1.1±0.3	1.8±0.4